A Correspondence Framework for ALS Strip Adjustments based on Variants of the ICP Algorithm

Philipp Glira, Norbert Pfeifer, Christian Briese & Camillo Ressl, Vienna, Austria

Abstract: In order to minimize discrepancies within the overlap area of airborne laser scanning (ALS) strips, strip adjustment can be performed. Apart from the transformation model, the quality of strip adjustment is strongly affected by the observations used in this process. In order to exploit the full resolution of the data, correspondences should be established on the basis of the original point cloud instead of interpolated surfaces or rasters, so that a loss in accuracy and systematic interpolation effects can be avoided. A surface matching method in which correspondences are based on the original point cloud is the iterative closest point (ICP) algorithm. In this study several ICP variants suitable for large amounts of data are investigated. We introduce a new method for the selection of correspondences which is based on the influence of a point on the adjustment calculations. As a result of this study, a combination of variants, forming a baseline optimized for most ALS data, is presented. The investigated variants provide a correspondence framework for ALS strip adjustment. The benefit of specific variants is demonstrated on the basis of a challenging ALS scene.

Zusammenfassung: *Korrespondenzen für die ALS-Streifenausgleichung auf Basis von ICP.* Durch eine Streifenausgleichung können systematische Diskrepanzen im Überlappungsbereich von Airborne Laser Scanning (ALS)-Streifen minimiert werden. Die Qualität einer Streifenausgleichung hängt neben dem Transformationsmodell wesentlich von den verwendeten Korrespondenzen ab. Nutzt man für die Korrespondenzen die Punktwolke selbst anstelle von interpolierten Flächen oder Rastern, so kann man davon ausgehen, keinen Genauigkeitsverlust oder systematischen Fehler durch Interpolationseffekte zu erleiden, und somit sehr hohe Genauigkeitsansprüche erfüllen zu können. Eine Methode, auf die das zutrifft, ist der Iterative Closest Point (ICP) Algorithmus. In dieser Arbeit wurden mehrere für große Datenmengen geeignete ICP-Varianten untersucht. Im Zuge dessen stellen wir eine neue Selektionsmethode für Korrespondenzen vor, die auf dem Einfluss jedes Punktes auf das Ausgleichsergebnis aufbaut. Als Ergebnis dieser Studie wird in diesem Artikel eine Variantenkombination vorgestellt, die für typische ALS-Szenen optimiert ist. Diese kann als Grundlage für die Korrespondenzbildung einer Streifenausgleichung herangezogen werden. Der Vorteil bestimmter Varianten wird anhand einer geometrisch herausfordernden ALS-Szene gezeigt.

1 Introduction

Airborne laser scanning (ALS) is the prime data acquisition method for digital terrain models (DTM), especially in forested areas or areas with little texture. In order to georeference the scanner raw measurements, the following information is required (Skaloud & Lichti 2006, Ressl et al. 2009):

1. The position and orientation of the acquisition platform. They are measured by a position and orientation system (POS), consisting of a GNSS system (global navigation satellite system) and an INS (inertial navigation system).

2. The relative orientation of the scanner to the POS, consisting of a rotational and a translational part (mounting calibration).
3. The time synchronization between scanner and the POS system.
4. Internal scanner parameters, e.g. zero point and scale of range and angle.

Any inaccuracy in these categories results in wrong coordinates of the ground points. In order to minimize and correct these systematic errors, a strip adjustment can be performed. One of the major challenges in this context is the necessity to handle large amounts of data, thus algorithms have to be fast and efficient. On the other hand, the initial orientations of the strips are typically relatively good, since systematic errors are small compared to the extents of the strips.

The basic observations for a strip adjustment are corresponding geometric elements, e.g. points or planes, within the overlap area of the strips. To exploit the full potential of ALS, these correspondences should be established on the highest data resolution level, i.e. on the basis of the original point cloud, as interpolation potentially introduces additional errors (Toth 2008). A surface matching method in which correspondences are based on the original point cloud is the iterative closest point (ICP) algorithm (Besl & McKay 1992, Chen & Medioni 1991).

The aim of the ICP algorithm is finding the optimal alignment of two overlapping point clouds. The geometric transformation applied within the ICP algorithm is typically a rigid body transformation. In ALS strip adjustment with trajectory information the transformation model is more complex (Skaloud & Lichti 2006). However, we are interested in the correspondence problem primarily. Therefore, we only concentrate on a single strip pair, whose alignment is an inherent part of ICP. The topic of strip adjustment is only briefly addressed.

We study the effects of different ICP variants on convergence speed and accuracy. A few variants are newly introduced to meet the special requirements in ALS. One of them addresses the problem of correspondence selection and is called "maximum leverage sampling". Using this new strategy the correspondences which are best suited for the estimation of the transformation are selected. All investigated variants are suitable for large amounts of data, as they typically occur in ALS.

After a review of related literature, the basic ICP concept is described, introducing a taxonomy of the algorithm in five main steps, derived from Rusinkiewicz & Levoy (2001). Next, the investigated variants for each of these steps are presented. In this context, a combination of variants forming a baseline optimized for most ALS data is introduced. We conclude by demonstrating the benefits of specific variants.

2   Related work

In the rich body of literature on ICP algorithms, a huge number of modifications were derived from the original works of Besl & McKay (1992) and Chen & Medioni (1991). They refer to the selection of points, the weighting of correspondences, the metric for measuring the distance, and other aspects. A summary has been given by Rusinkiewicz & Levoy (2001), who suggest that a better expansion of the acronym ICP would be iterative *corresponding* point instead of the original iterative closest point. Planitz et al. (2005) summarize methods based on intrinsic surface parameters for solving the correspondence problem. References to ICP variants adopted for this study are given in section 5.

Strip adjustment methods are either formulated in a rigorous way, i.e. with trajectory and calibration parameters, (Kager 2004, Skaloud & Lichti 2006, Kerstling et al. 2012) or in an approximate way, i.e. without trajectory (Ressl et al. 2009). The strip discrepancies can be minimized in a pairwise way or simultaneously for all strip pairs. Correspondences are either generated on the basis of the original point cloud or of derived data, e.g. a grid, a triangulation or higher order primitives (Maas 2002). Most approaches use planes as corresponding features. They can be of fixed or variable size, in the latter case determined by segmentation (Pfeifer et al. 2005, Filin & Vosselman 2004). In Akca (2010) reflectance, colour and temperature are considered as additional input for the matching of point clouds.

An overview of strip adjustment methods is given by Toth (2008).

3   General ICP Concept and Taxonomy

The ICP algorithm improves the alignment of two point clouds by minimizing the discrepancies within the overlap area of these point clouds. The alignment is optimized by transforming iteratively the so called loose point cloud, whereas the position of the other point cloud remains fixed. To apply the algorithm, a good estimate of the initial relative orientation of the point clouds is necessary. This main requirement is typically fulfilled in ALS.

The ICP algorithm can be broken down into five main steps (Fig. 1):
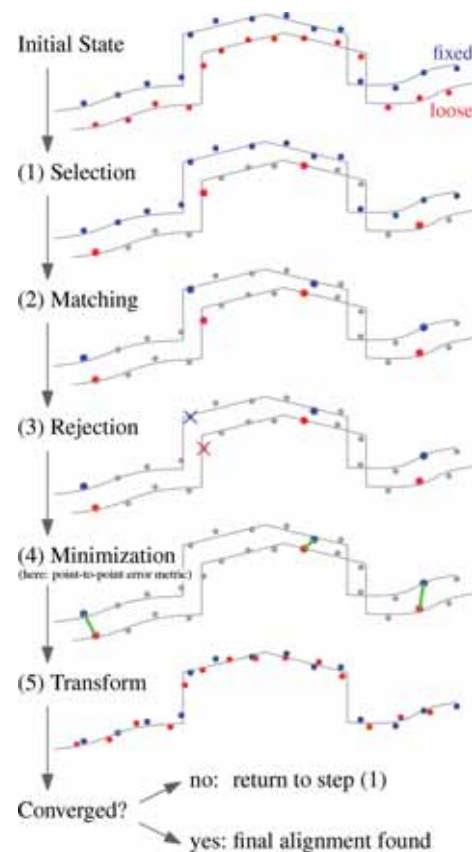
Fig. 1: Visualization of the five basic ICP steps for two overlapping strips (blue = fixed strip, red = loose strip, green = correspondence).

1. **Selection**
   A subset of points is selected within the overlap area in one point cloud.
2. **Matching**
   Find the corresponding points of the selected subset in the other point cloud.
3. **Rejection**
   False correspondences (outliers) are rejected on the basis of the compatibility of points.
4. **Minimization**
   Estimation of transformation parameters (for the loose point cloud) by minimizing the distances between corresponding points.
5. **Transformation**
   Transformation of the loose point cloud using the estimated parameters.

Finally, a suitable convergence criterion is tested. If it is not met, the process restarts from step 1, or step 2 if point selection is not repeated iteratively. In section 5 we will discuss some variants for each of these five steps.

4   Preprocessing of the ALS Data

The surface normal vectors of the point clouds are required many times throughout the alignment process (section 5). Therefore, the preprocessing of the ALS data includes the estimation of the normal vector $\boldsymbol{n} = (n_x\, n_y\, n_z)^T$ ($\|\boldsymbol{n}\| = 1$) and its reliability for each point.

The surface normal vectors can be estimated for each point using a principal component analysis of the co-variance matrix of the co-ordinates of neighbouring points (Shakarji et al. 1998). It is recommended to select a neighbourhood based on a fixed radius search, where the search radius should be chosen in dependence of (a) the point density and (b) the topography of the strips. Considering the point density in selecting the search radius should ensure that a sufficient number of neighbouring points is used for the normal vector estimation, e.g. $n \geq 8$, whereas the topography has to be considered so that the radius does not exceed the size of the available smooth surface areas. Usually, we choose the search radius in the range of 1 m – 3 m. Given this set of n three dimensional points,
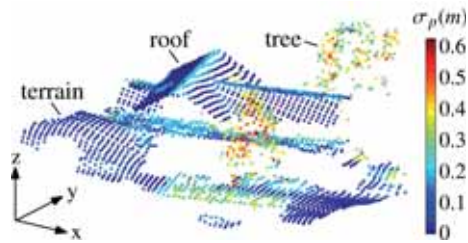
Fig. 2: ALS point cloud coloured by the roughness attribute σ_p. For the alignment process only points in smooth areas should be used, e.g. points with $\sigma_p \leq 0.1$ m.

$\mathbb{P} = \{\boldsymbol{p}_1, \boldsymbol{p}_2, \boldsymbol{p}_3, ..., \boldsymbol{p}_n\}, \boldsymbol{p} \in \mathbb{R}^3$, the 3×3 co-variance matrix of its co-ordinates is denoted by $\boldsymbol{C}(\mathbb{P})$. The principal components of $\boldsymbol{C}(\mathbb{P})$ are its eigenvectors and form an orthogonal basis. The associated eigenvalues correspond to the variance in the directions of the eigenvectors. Assuming a descending ordering of the eigenvalues ($\lambda_1 \geq \lambda_2 \geq \lambda_3$), the third eigenvector $\boldsymbol{e}_3$ is a least-squares estimate for the normal vector of the adjusting plane ($\boldsymbol{n} = \boldsymbol{e}_3$). The square root of the third eigenvalue can be used as a reliability measure for the normal vector. This value corresponds to the standard deviation of the selected points from the estimated plane and can therefore be interpreted as a measure for the roughness of the adjusting plane ($\sigma_p = \sqrt{\lambda_3}$) (Fig. 2).

To ensure a high reliability of the normal vectors, only points on smooth surface areas should be retained for the alignment process, e.g. $\sigma_p \leq 0.1$ m.

Each of these remaining points is then described for the subsequent steps by its co-ordinates $\boldsymbol{p} = (x \ y \ z)^T$, its normal vector $\boldsymbol{n} = (n_x \ n_y \ n_z)^T$ and its roughness measure σ_p.

5   ICP Variants Suitable for ALS Data

This section covers some variants of the ICP algorithm for each of the steps introduced in section 3. A special focus lies on the applicability on large amounts of data, as they typically occur in ALS. The new proposed selection method called **maximum leverage sampling** is briefly introduced here. A detailed description follows in section 6.

Variants forming a **baseline optimized for most ALS scenes** are marked by an asterisk **(*)**.

5.1 *Selection (Step 1)*

For comparatively small point clouds each point may be selected. However, for ALS data this is not feasible. This is particularly true if the single strip pair problem is generalized to an ALS strip adjustment of a complete data acquisition campaign, in which hundreds of strip pairs have to be processed simultaneously. Thus, compared to the full amount of available data (up to several million points), only a comparatively small number (a few thousands) of points can be selected within the overlap area of each strip pair. Since the selected subset heavily affects the final alignment accuracy, the selection of relevant points is crucial.

We consider the following four strategies for the selection of points in one point cloud. They are sorted by increasing computational complexity (Fig. 3):

1. Random sampling

This is the fastest of the investigated options: points are randomly selected within the overlap area (Masuda & Yokoya 1995). Since the point density of ALS is only varying slightly, compared e.g. to typical TLS datasets, this option can be considered as an approximation of uniform sampling.

2. Uniform sampling

Uniform sampling in object space gives a homogeneous distribution of the selected points within the overlap area. This option was implemented by dividing the overlap area into a voxel structure and selecting the closest point to each voxel centre. Consequently, the mean sampling distance in each coordinate direction corresponds to the edge length of a single voxel. A k-d tree was used for the closest point search.
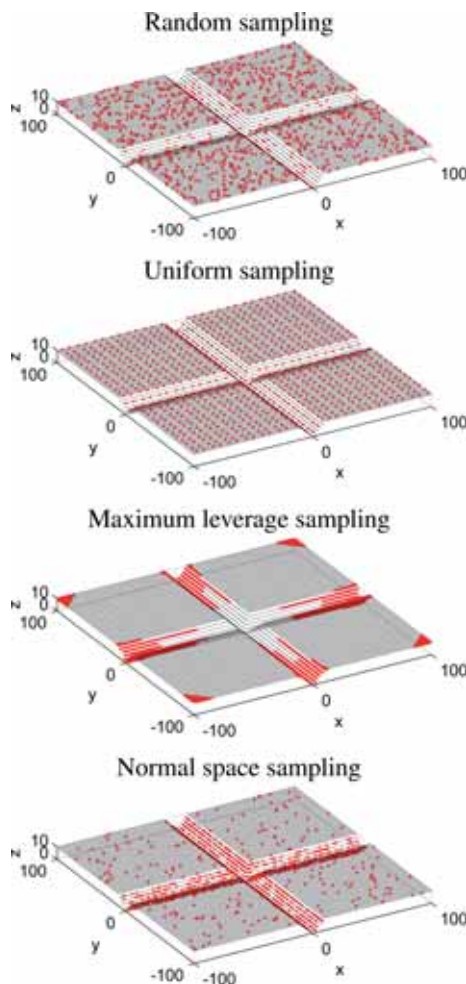
3. Maximum leverage sampling (*)

This strategy selects those points which are best suited for the estimation of the transformation parameters. For this purpose, the leverage of each point on the parameter estimation is considered. This method is described in section 6.

4. Normal space sampling

The aim of this strategy is to select points such that the distribution of their normals in angular space is as uniform as possible (RUSINKIEWICZ & LEVOY 2001). For this the angular space (slope vs. aspect) is divided into classes, e.g. $2.5° \times 10°$, and points are randomly sampled within these classes. Strategies 3 and 4 are useful when one normal direction is predominating, but the data still include some valuable features for the alignment. This is especially true for ALS data acquired over flat terrain.

A comparison of the methods is shown in Fig. 3. For this figure, a synthetic point cloud made of 10,201 points ($=101^2$) was generated by sampling a plane with two orthogonal ditches. For each strategy 10% of the original points were selected.

5.2 *Matching (Step 2)*

In this step the correspondences are established, i.e. each selected point from the previous step is matched with one point in the other point cloud.

The simplest strategy is to match the selected points to their **closest points (*)**, as proposed by BESL & McKAY (1992). We found that for ALS data this is an adequate choice, mainly due to the good initial relative orientation and the high point density of ALS strips. The search for closest points can be realized efficiently using k-d trees.

Further matching methods are either computationally too expensive, e.g. **normal shooting**, (CHEN & MEDIONI 1991), **reverse calibration** (BLAIS & LEVINE 1995), or not necessary (PLANITZ et al. 2005) due to the good initial orientation of the strips, e.g. **closest compatible point** (SHARP et al. 2002). Thus, within this study, no other variants were investigated for this step.

Fig. 3: Comparison of different selection strategies. With each strategy 10% of points are selected.

5.3 *Rejection (Step 3)*

The aim of this step is the a priori detection and rejection of false correspondences (outliers), as they may have a large effect on the result of the minimization step. One option is the **rejection on the basis of the distances between corresponding points (*)**. For this strategy the distribution of the a priori distances between corresponding points is analyzed. For the recommended point-to-plane error metric (see next step), the signed distances $d_1, d_2, ..., d_n$ are assumed to have a Gaussian distribution. A robust estimator for the standard deviation (HAMPEL 1974) of this contaminated normal distribution is given by

$$\sigma_{mad} = 1.4826 \cdot mad, \qquad (1)$$

where mad is the median of the absolute differences (with respect to the median)

$$\text{mad} = \text{median}_i \left(\left| d_i - \text{median}_j (d_j) \right| \right). \qquad (2)$$

In this work, all correspondences with distances outside the range

$$d_{\max} = \tilde{d} \pm 3\sigma_{\text{mad}} \qquad (3)$$

are rejected, where $\tilde{d}$ denotes the median of the point-to-plane distances.

Another option is the **rejection based on the angle between the normal vectors of corresponding points (*)**. The angle between the normals of two corresponding points *p* and *q* is defined as:

$$\alpha = \text{acos}(\boldsymbol{n}_p^T \cdot \boldsymbol{n}_q). \qquad (4)$$

To ensure that two corresponding points belong to the same plane, e.g. a roof, we recommend to reject all correspondences with α larger than

$$\alpha_{\max} = 5°. \qquad (5)$$

Additionally, **a rejection based on additional attributes of corresponding points** can be performed if invariant attributes are available for the ALS points. For example, if reflectance values are available, false corresponding points can possibly be detected by comparing their reflectance values.

It is recommended to apply all of the presented rejection strategies. However, it is not guaranteed that this will lead to an a priori rejection of all outliers in the observation data. Thus, a robust adjustment method is used for the detection and removal of the remaining ones.

5.4 *Minimization (Step 4)*

The transformation parameters are usually estimated by minimizing the sum of squared distances between the established correspondences. Two types of distances are commonly used (Fig. 4).

1. Euclidean (unsigned) distance between corresponding points ("**point-to-point" error metric** Δs) (Besl & McKay 1992):

The objective function to be minimized is

$$E = \sum_i \Delta s_i^2 = \sum_i \left\| T(\boldsymbol{p}_i) - \boldsymbol{q}_i \right\|^2 \qquad (6)$$

where $\boldsymbol{p}_i$ and $\boldsymbol{q}_i$ are the corresponding points, and T denotes a transformation. The fixed point cloud is formed by the points $\boldsymbol{q}_i$ and the loose point cloud by the points $\boldsymbol{p}_i$.

This error metric should be avoided in ALS, because due to the different ground sampling of two ALS strips, no real point-to-point correspondences exist and the convergence speed is somewhat slow (Rusinkiewicz & Levoy 2001). If a rigid-body transformation is applied, a closed form solution exists for this error metric (Horn et al. 1998).

2. Perpendicular (signed) distance of one point to the tangent plane of the other point ("**point-to-plane" error metric** Δp) (*) (Chen & Medioni 1991):

The objective function to be minimized is:

$$E = \sum_i \Delta p_i^2 = \sum_i \left[\left(T(\boldsymbol{p}_i) - \boldsymbol{q}_i \right)^T \cdot \boldsymbol{n}_i \right]^2, \qquad (7)$$

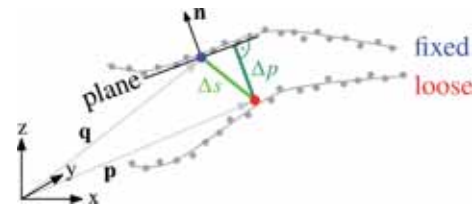where $\boldsymbol{n}_i$ are the normal vectors in $\boldsymbol{q}_i$.

Fig. 4: Comparison of point-to-point (Δs) and point-to-plane (Δp) error metric.

In contrast to the point-to-point error metric, for this error metric it is not necessary for the corresponding points to be identical in object space. The only requirement is that the corresponding points belong to the same plane in object space, e.g. roof. This error metric is characterized by a high convergence speed, as flat regions can slide along each other without costs, i.e. without increasing the value of the objective function *E*. A closed form solution exists for the rigid-body transformation only after linearizing the rotation matrix, i.e. for small rotations (Chen & Medioni 1991).

In this study, the optimization problem was solved using the Gauss-Markov adjustment model, also called least-squares adjustment by indirect observations. Outliers were detected by using adaptive weights within the adjustment (KRAUS 1997). The closed form solutions were used for verification.

5.5 *Transformation (Step 5)*

Using a **rigid body transformation** with 6 parameters for rotation and translation for improving the relative and absolute orientation of ALS strips appears to be a reasonable choice. However, as pointed out in RESSL ET AL. (2009), if additionally the effects of a wrong mounting calibration shall be reduced without considering the GNSS-INS trajectory data, then it is important to use an **affine transformation** with 12 parameters.

Reformulating (7) the objective function to be minimized for the recommended point-to-plane error metric is

$$E = \sum_i \left[(R\,\boldsymbol{p}_i + \boldsymbol{t} - \boldsymbol{q}_i)^T \cdot \boldsymbol{n}_i \right]^2, \tag{8}$$

where $\boldsymbol{t}$ denotes a 3-by-1 translation vector and R denotes a 3-by-3 orthogonal rotation matrix for the rigid-body transformation or a 3-by-3 affine matrix for the affine transformation.

6 Maximum Leverage Sampling

The quality of the parameter estimation depends heavily on the selected subset of points (step 1). For example, if too many correspondences are situated in featureless regions, the ICP algorithm may fail to converge because of lack of constraints. Here we propose a new method for the selection of points, which minimizes the uncertainty of the estimated transformation parameters. That is, we select the points which provide the strongest constraints on the transformation. As a consequence, a very small number of correspondences is sufficient for the alignment of two ALS strips. This is of particular advantage when hundreds of strip pairs have to be processed simultaneously within a strip adjustment.

We start from some basic formulae of the Gauss-Markov adjustment model. Then we derive the hat matrix H on which the presented method is based, including some brief explanations of its properties. Subsequently, an example of the hat matrix for a specific case (point-to-plane error metric and rigid body transformation model) is given. Finally, the point selection algorithm is presented.

6.1 *The Hat Matrix H*

We consider a system of linear equations given by

$$\boldsymbol{l} \approx A\boldsymbol{x}, \tag{9}$$

where the u unknown transformation parameters $\boldsymbol{x}$ are linked with the n original observations $\boldsymbol{l}$ by the full-column rank n-by-u coefficient matrix A. This over-determined equation system ($n > u$) is solved by introducing n residuals $\boldsymbol{v}$ for the observations $\boldsymbol{l}$

$$\boldsymbol{l} + \boldsymbol{v} = A\hat{\boldsymbol{x}} \tag{10}$$

and minimizing the least-squares objective function $E = \boldsymbol{v}^T\boldsymbol{v}$. By substituting $\boldsymbol{v}$ with $A\hat{\boldsymbol{x}} - \boldsymbol{l}$ and setting the partial derivatives $\partial E / \partial \hat{\boldsymbol{x}} = 0$ the estimates for the parameters $\hat{\boldsymbol{x}}$ are determined by

$$\hat{\boldsymbol{x}} = (A^T A)^{-1} A^T \boldsymbol{l}. \tag{11}$$

The unknown rms-error of the weight unit $\hat{\sigma}_0$ can be estimated by

$$\hat{\sigma}_0 = \sqrt{\frac{\boldsymbol{v}^T\boldsymbol{v}}{n-u}}. \tag{12}$$

The covariance matrix $\sum_{\hat{x}\hat{x}}$ of the estimated unknown parameters $\hat{\boldsymbol{x}}$ is then given by

$$\Sigma_{\hat{x}\hat{x}} = \hat{\sigma}_0 Q_{\hat{x}\hat{x}}, \tag{13}$$

$$Q_{\hat{x}\hat{x}} = (A^T A)^{-1}. \tag{14}$$

If we denote the estimated observations by $\hat{\boldsymbol{l}} = \boldsymbol{l} + \boldsymbol{v}$, (10) can be rewritten together with (11) as

$$\hat{l} = A(A^T A)^{-1} A^T l. \tag{15}$$

To emphasize the fact that each $\hat{l}_i$ is a linear combination of the original observations l, (15) can be written as

$$\hat{l} = Hl, \tag{16}$$

with

$$H = A(A^T A)^{-1} A^T. \tag{17}$$

The n-by-n matrix H is known as the **hat matrix**, as it "puts a hat on l". On the one hand H is a projection matrix, as it projects l into $\hat{l}$. On the other hand H describes the amount of leverage or influence each observed value in l has on each fitted value in $\hat{l}$. For instance, the i-th row of H contains the influence of the original observations l on the estimated observation $\hat{l}_i$. More precise, the element h_{ij} can be interpreted as the influence of the observation l_j on $\hat{l}_i$. This value is independent from the actual value of l_j, because for uncorrelated and unweighted observations H only depends on A.

Due to these properties, the hat matrix can be used to identify observations which have a large influence on the parameter estimation. Such influential observations are defined according to BELSLEY et al. (1980) as:

"An influential observation is one which, either individually or together with several other observations, has a demonstrably larger impact on the calculated values of various estimates (…) than is the case for most of the other observations."

For a specific observation l_i the influence on the parameter estimates is most directly reflected in its leverage on the corresponding estimated observation $\hat{l}_i$ (HOAGLIN & WELSCH 1978). This information is precisely contained in the corresponding diagonal element h_{ii} of the hat matrix. Thus, we focus our analysis on the diagonal elements of H, the so called **leverages**. They can be directly computed by

$$h_{ii} = a_i (A^T A)^{-1} a_i^T, \tag{18}$$

where a_i denotes the i-th row of A. In this way the memory-intensive computation of the off diagonal elements of H can be avoided.

The leverages have two important properties. According to HOAGLIN & WELSCH (1978) for the leverages h_{ii} it holds that

$$0 \le h_{ii} \le 1. \tag{19}$$

Further, as a projection matrix, H is symmetric and idempotent ($H^2 = H$). The trace of an idempotent matrix is equal to its rank, i.e. trace(H) = rank(H). From (17), it can be seen that rank(H) = rank(A) = u, and hence trace(H) = u, i.e.

$$\sum_{i=1}^{n} h_{ii} = u, \tag{20}$$

where u denotes the number of parameters. The redundancy numbers, which are commonly used in adjustment theory, are linked to the leverages by

$$r_{ii} = 1 - h_{ii}. \tag{21}$$

According to FÖRSTNER (1979), the redundancy number describes the contribution of a single observation to the overall redundancy $r = n - u$, i.e. $\sum_{i=1}^{n} r_{ii} = r$.

A side note about **partial leverages**: The leverages discussed so far are relevant when all parameters are of equal interest. However, an observation may be influential only for one or a few parameters. For instance, a point on horizontal terrain is especially important for the estimation of the vertical component of the translation vector, but at the same time it is entirely redundant for the estimation of its horizontal components. Thus, the partial influence of an observation on a single parameter may be of interest. It is given by the partial leverages.

The partial leverage $h_{j,i}$ describes the influence of the i-th observation on the estimation of the j-th parameter and is defined according to CHATTERJEE & HADI (1986) as

$$h_{j,i} = \frac{v_{j,i}^2}{v_j^T v_j} \tag{22}$$

$$v_j = (I - H_{[j]}) A_j \tag{23}$$

with I n-by-n identity matrix,
     $H_{[j]}$ hat matrix calculated by omitting the j-th column of A,
     A_j j-th column of A,
     $v_{j,i}$ i-th element of $\mathbf{v}_j$.

As their name already implies, the sum of the partial leverages of an observation gives its overall leverage

$$h_{ii} = \sum_{j=1}^{u} h_{j,i} \ . \tag{24}$$

To be complete, in presence of a weight matrix $P = Q_{ll}^{-1}$ for the observations based on a covariance matrix Q_{ll}, the hat matrix becomes

$$H = A(A^T P A)^{-1} A^T P, \tag{25}$$

i.e. H depends on A and P. If the observations are correlated, i.e. the weight matrix P is not a diagonal matrix, the leverages are not restricted to the range [0,1].

6.2 *Leverage Calculation Example*

Let us assume the point-to-plane error metric (step 4) and the rigid body transformation model (step 5) were chosen for the alignment of two ALS strips. Due to the good initial relative orientation of the point clouds, the rotation matrix R can be linearized, substituting $\cos(\alpha) \approx 1$ and $\sin(\alpha) \approx \alpha$. Thus (8) can be written as

$$E = \sum_i \left[\left(\boldsymbol{p}_i + \boldsymbol{r} \times \boldsymbol{p}_i + \boldsymbol{t} - \boldsymbol{q}_i \right)^T \cdot \boldsymbol{n}_i \right]^2 , \tag{26}$$

where $\boldsymbol{r} = (\alpha_x \ \alpha_y \ \alpha_z)^T$ is the vector containing the rotation angles about the x, y, and z axes, respectively, and $\boldsymbol{t} = (t_x \ t_y \ t_z)^T$ is the translation vector. After a few algebraic steps, the n-by-6 coefficient matrix A can be found for $\boldsymbol{x}^T = (\boldsymbol{r}^T \ \boldsymbol{t}^T)$ as
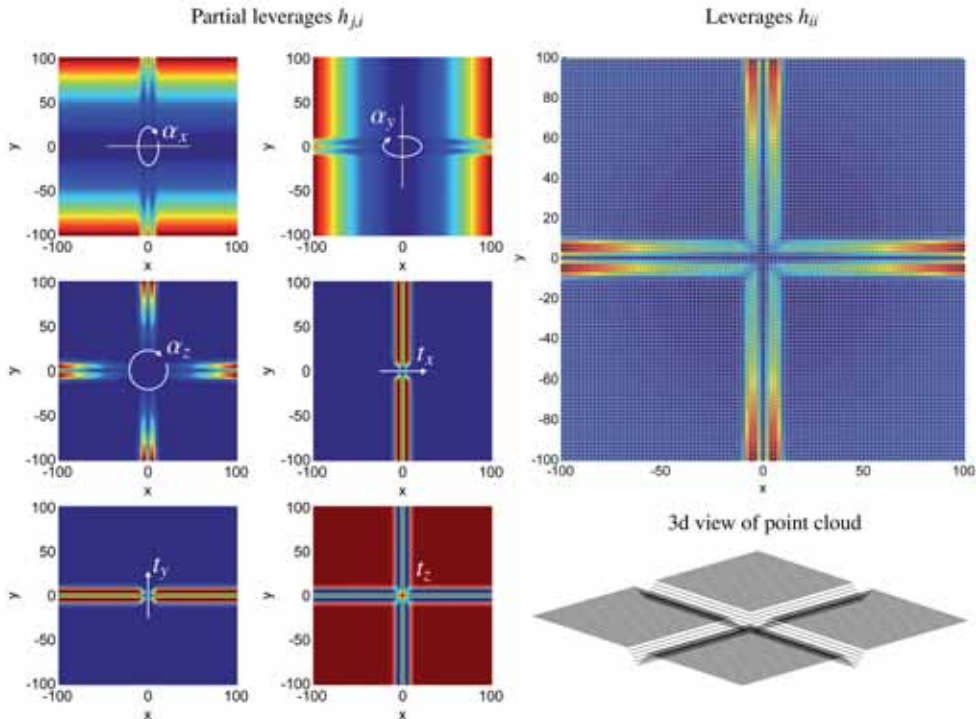
Fig. 5: Partial leverages (left) and leverages (right) of the synthetic point cloud introduced in Fig. 3. (red = high leverage, blue = low leverage).

$$A = \begin{pmatrix} (\boldsymbol{p}_1 \times \boldsymbol{n}_1)^T & \boldsymbol{n}_1^T \\ (\boldsymbol{p}_2 \times \boldsymbol{n}_2)^T & \boldsymbol{n}_2^T \\ \vdots & \vdots \\ (\boldsymbol{p}_n \times \boldsymbol{n}_n)^T & \boldsymbol{n}_n^T \end{pmatrix}. \tag{27}$$

As can be seen, each point $\boldsymbol{p}_i$ contributes one row to A, i.e. it corresponds to one observation. It is clear that not all of the points have an equal importance in the least-squares adjustment. Thus, with (18) the leverage $\boldsymbol{h}_{ii}$ of each point $\boldsymbol{p}_i$ can be computed. This tells us how much influence a point $\boldsymbol{p}_i$ has on the estimation of the transformation parameters. If the estimation of the leverages should rely exclusively on the points $\boldsymbol{p}_i$, the normals in (27), which according to (7) belong to the points $\boldsymbol{q}_i$, can be replaced by the normals of $\boldsymbol{p}_i$ due to (5).

In Fig. 5 the partial leverages and the leverages are visualized for the synthetic point cloud introduced in section 5.1. It can be clearly seen that the partial leverages (left) identify those points which are most influential for the estimation of a single transformation parameter. For instance, for the rotation parameter α_x, points with larger distances from the rotation axis x are more influential than points next to it. The leverages (right), as the sum of the partial leverages, represent the influence of each point on the simultaneous estimation of all six transformation parameters. As expected, the points in the ditches and at the edges of the point cloud have the largest impact on the parameter estimation.

Summarizing the contents of this section, the diagonal elements of the hat matrix, called leverages, describe the influence of an observation on the parameter estimation. For uncorrelated and unweighted observations, the hat matrix can be calculated exclusively from the coefficient matrix A, see (17). Otherwise, the weight matrix P is also necessary, see (21). Since in the ICP algorithm each point corresponds to one observation, the leverages can be used to describe the influence of each point on the estimation of the transformation parameter. In the next section we show how points are selected on the basis of this information.

6.3 *The Selection Algorithm*

Usually the leverages are used for the identification of potential blunders in the observation data. However, we use the leverages to identify those points which are best suited for the estimation of the transformation parameters, i.e. have the largest impact on the parameter estimation. In terms of redundancy numbers (21), the points with the lowest redundancy are selected. This selection of points with low redundancy does not pose a problem on the identification of blunders within a robust adjustment. Because of the high overall redundancy in the ICP algorithm (hundreds of observations vs. few transformation parameters) the redundancy of the selected high leverage points is still very high: In the examples considered in this article the redundancy of these selected points is still always above 0.99. The following scheme provides a description of the algorithm.

Algorithm **Maximum leverage sampling**

Input:
   Point cloud: $\mathbb{P} = \{\boldsymbol{p}_1, \boldsymbol{p}_2, ..., \boldsymbol{p}_n\}$
   Normals: $\mathbb{N} = \{\boldsymbol{n}_1, \boldsymbol{n}_2, ..., \boldsymbol{n}_n\}$
   No. of points to select: m
Initialize vector with indices of all points:
$\boldsymbol{s} = (1 \ 2 \ ... \ n)^T$
Compute coefficient matrix A
while rows(A) > m **do**

   $Q_{\hat{x}\hat{x}} = (A^T A)^{-1} \tag{14}$

   for i = 1 to rows(A) **do**

      $h_{ii} = \boldsymbol{a}_i Q_{\hat{x}\hat{x}} \boldsymbol{a}_i^T \tag{18}$

   end for
   Find index j of point with lowest h_{ii}:
   j = find(min(h_{ii}))
   Delete row $\boldsymbol{a}_j$ from A
   Delete j-th element from $\boldsymbol{s}$
end while
Return $\boldsymbol{s}$ with indices of selected points

The selection algorithm starts with the indices of all n points in a vector $\boldsymbol{s}$, i.e. at the beginning all points are selected. Based upon this, the points with the lowest leverages are removed iteratively from $\boldsymbol{s}$ until m points are left. Please note that due to the

correlation of the leverages (17) one cannot simply select m points after the first computation of the leverages, but they have to be recomputed in each iteration.

To speed up the algorithm, instead of removing only one single point, the k points with the lowest leverages may be removed from s in each iteration. We found out empirically that for relatively small values of k, e.g. $k = 10$, this has a negligible effect on the final selection of points, but it leads to a substantial reduction in processing time.

7   Experimental Results

In this section, the introduced correspondence framework is demonstrated on the basis of synthetic ALS data. The motivation for using synthetic data is that the correct orientation is known exactly, and the correctness of the estimated transformations can be evaluated relative to this "ground truth" orientation. A digital elevation model (DEM) of the selected ALS scene, which consists primarily of almost flat terrain intersected by a narrow ditch, is shown in Fig. 6. This dataset was chosen because it is a rather difficult scene for most ICP variants, as there is only one feature - the ditch - which can constrain the transformation at the finest level. Thus, this dataset is used to emphasize the differences between the presented variants.

The two synthetic point clouds were generated by the following steps:
1. Extraction of a 1000 m × 100 m area from a real ALS strip.

2. Derivation of a DEM from this point cloud (least-squares moving planes interpolation, grid size = 0.5 m).
3. Generation of the two synthetic ALS strips: bilinear interpolation of the DEM at randomly distributed positions in the xy plane for each of the two point clouds (mean point density = 4 points/m^2). Consequently, each strip consists of 400,000 points.
4. Transformation of one of the two point clouds by a rigid body transformation. For the first two experiments (section 7.1 and 7.2) a translation vector $t = (0.5\ 0.5\ 0.5)^T$ m and a rotation about the z axis with $\alpha_z = 0.1°$ were chosen. This leads to point displacements at the edges of the point cloud of about 1 m, which is far more than usual displacements between real ALS strips. For the third experiment (section 7.3), each of the 6 transformation parameters was varied within a specific range, whereas the other 5 transformation parameters were set to zero.

The ICP algorithm tries to bring back the transformed point cloud to its original position. After each iteration, for each point the Euclidean distance between its current position and its original position can be computed. We denote the root-mean-square of these distances as *alignment error* and use this error metric for the comparison of different ICP variants. The rigid body transformation (3 rotations, 3 translations) was chosen as the transformation model. The proposed **baseline method**, marked by an asterisk **(*)** throughout this document, is applied for all steps which are *not* under investigation in the subsequent examples.
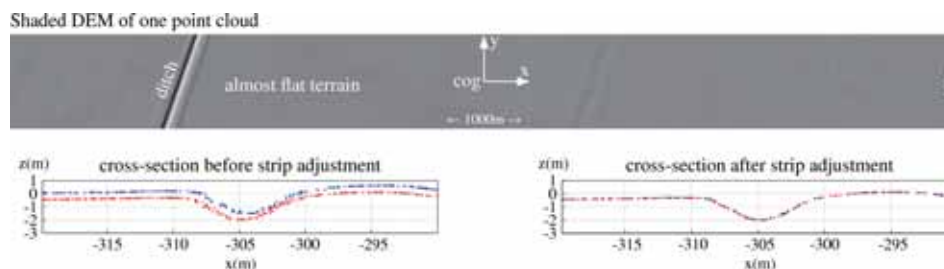
Fig. 6: Top: digital elevation model of ALS test scene, bottom: cross-section through ditch before and after the strip adjustment.

7.1 *Comparison of Selection Strategies*

First, we examine the effect of the selection strategies introduced in section 5.1 on the convergence of the ICP algorithm. For this purpose, with each strategy about 300 points (or 0.075% of all points) are selected for the estimation of the 6 transformation parameters.

As can be seen in Fig. 7, using **random sampling (RS)** and **uniform sampling (US)**, most of the points are selected in flat regions, containing a lot of redundant information for the alignment process. From these points the translation in x and y, as well as the rotation about the z axis can hardly be estimated. For

these 3 parameters, points within the ditch would be most useful, but as these strategies do not focus on local terrain features, only a few points are selected within this area.

However, **normal sampling (NS)** and **maximum leverage sampling (MLS)** consider the usefulness of points for the alignment process. Especially the MLS strategy selects the points with the highest leverage on the estimation of the transformation parameters. Thus, for the test scene, points are predominantly selected within the ditch and, in order to constrain the rotation about the ditch axis, in a direction perpendicular to it. It can also be recognized that the algorithm prefers points near the edges, as they better constrain the transformation.
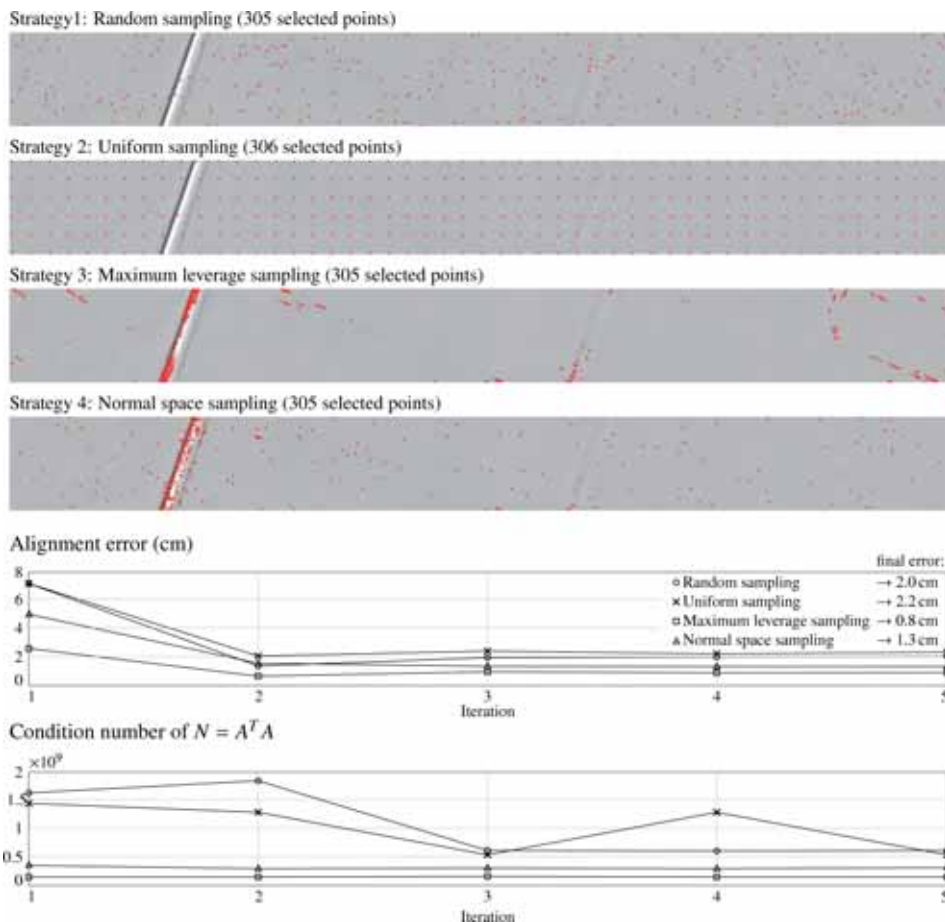
Strategy1: Random sampling (305 selected points)

Strategy 2: Uniform sampling (306 selected points)

Strategy 3: Maximum leverage sampling (305 selected points)

Strategy 4: Normal space sampling (305 selected points)

Alignment error (cm)

Condition number of $N = A^T A$

Fig. 7: Effect of different correspondence selection strategies on convergence and condition number.

Tab. 1: Precision of estimated transformation parameters for different sampling strategies in first ICP iteration. RS = random sampling, US = uniform sampling, MLS = maximum leverage sampling, NS = normal sampling.

|	translation (mm)			rotation (″) = 1/3600°		
	σ_{t_x}	σ_{t_y}	σ_{t_z}	σ_{α_x}	σ_{α_y}	σ_{α_z}
RS	38.0	29.6	0.3	0.033	0.003	0.410
US	30.5	23.8	0.2	0.024	0.003	0.314
MLS	11.5	22.2	0.6	0.059	0.007	0.261
NS	17.8	47.9	0.7	0.079	0.009	0.661

The convergence of the ICP algorithm for different selection strategies can be compared in Fig. 7. As stated above, the results are based on the point-to-plane-distance. One can see that with RS and US the convergence rate is rather slow and, even worse, the final *alignment error* is 2–3 times larger than with MLS. NS performs relatively well, but since points are not selected optimally, the final error is considerably larger than with MLS. The point selection does not only influence the convergence of the ICP algorithm, but also the a posteriori stochastic of the parameters. The standard deviations of the transformation parameters for the first ICP iteration can be compared in Tab. 1. For further iterations, the ratios between different selection strategies remain similar. This is also confirmed by a comparison of the condition numbers of the normal equation matrix $N = A^T A$, which indicate if the equation system is ill-conditioned (high condition number) or well-conditioned (low condition number).

7.2 *Comparison of Error Metrics*

In section 5.4 the point-to-point and point-to-plane error metric were introduced. As shown in Fig. 8, the convergence speed of the point-to-point error metric is very slow, and even for a good initial alignment many ICP iterations are necessary until the final alignment is reached. However, with the point-to-plane metric flat regions can slide along each other within one iteration without causing costs and therefore the speed of convergence is improved dramatically.

7.3 *Convergence Analysis*

The errors to be minimized by strip adjustment typically have magnitudes of up to a few decimetres. Only in exceptional cases the displacements of ALS strips are affected by gross errors, e.g. due to an accidentally wrong processing of the trajectory. Such errors can cause point displacements in the range of several metres. In this experiment we tried to find out if the presented method converges also with such bad initial orientations, and if so, how many iterations are necessary until the global minimum is reached. For this purpose, each of the six transformation parameters was varied (for the transformation of one point cloud, see section 7, step 4) within a specific range, whereas the remaining five parameters were set to zero. For each transformation parameter the range limits were selected so that they cause maximum point displacements of about 10 m. In Fig. 9 the numbers of iterations which are necessary to reach an *alignment error* smaller than 1 cm (stop criterion) are reported for each experiment. For example, for $t_x = 6$ m (and $t_y = t_z = \alpha_x = \alpha_y = \alpha_z = 0$) the presented method needs 7 iterations to reach the
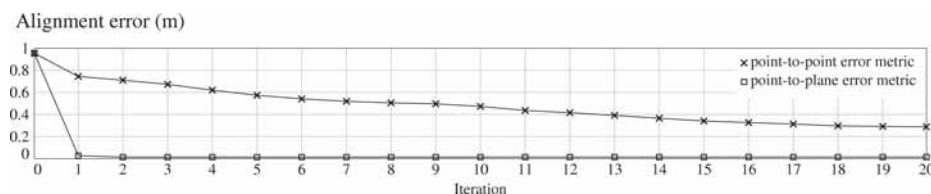
Fig. 8: Effect of different error metrics on the convergence of the strip adjustment. The results are based on uniform sampling for point selection.

stopping criterion. It can be seen that even for this difficult scene, all adjustments converged to the right solution. However, it should be noted that if the initial alignment is very bad, a relatively high number of iterations can be necessary, e.g. 9 iterations for $t_x = -10$ m. In our experience, gross errors in ALS data are always far below the selected range limits and therefore a divergence of strip adjustment can almost be ruled out as long as there are enough terrain features to constrain the transformation.
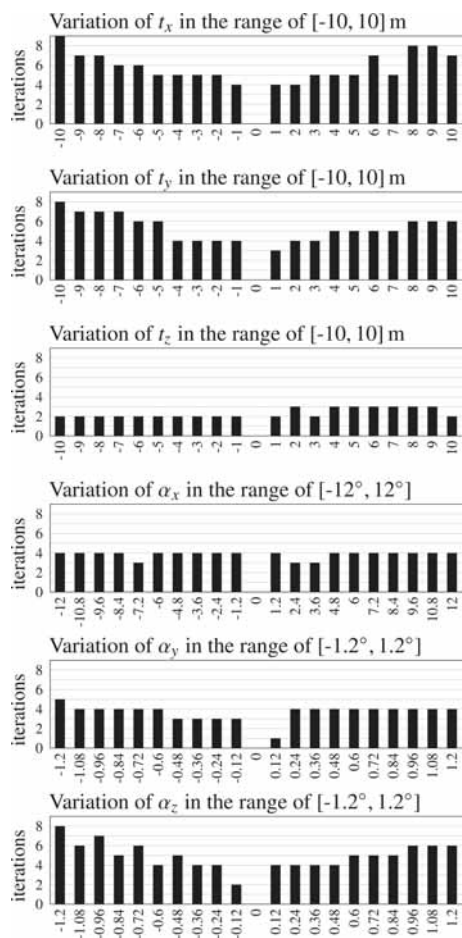

Fig. 9: Convergence analysis by variation of transformation parameters.

8   Conclusions and Outlook

This article presents a study of different options for ALS strip adjustment. A baseline of variants optimized for most typical ALS datasets was found by the comparison of several variants. The main findings of this work are:

- Correspondences have to be established carefully, because they have a large effect on the final alignment and the convergence speed of the strip adjustment. Within this study a new selection method called maximum leverage sampling was introduced, which considers the usefulness of points for the alignment process. This leads to a higher convergence rate and a better condition number of the normal matrix in the ICP algorithm.
- No real point-to-point correspondences exist in ALS data. This fact has to be considered by minimizing the distances between points and their corresponding tangent plane (instead of minimizing point-to-point distances).
- As the initial relative orientation of point clouds in ALS is typically quite good, only few iterations (< 5) are necessary in order to reach the global minimum of the error function. A divergence of the strip adjustment is very unlikely even if strips are affected by gross errors.

The correspondence framework presented here is already integrated in the module **ICP** of the software package **OPALS** (www.geo.tuwien.ac.at/opals). Currently we are working on the rigorous formulation of the strip adjustment problem, i.e. with the consideration of the trajectory information (SKALOUD & LICHTI 2006).

Acknowledgements

References

Akca, D., 2010: Co-registration of Surfaces by 3D Least Squares Matching. – Photogrammetric Engineering and Remote Sensing **76** (3): 307–318.

Belsley, D.A., Kuh, E. & Welsch, R.E., 1980: Regression Diagnostics: Identifying Influential Data and Sources of Collinearity. – Wiley, New York, NY, USA.

Besl, P. & McKay, N., 1992: A Method for Registration of 3-D Shapes. – Transactions on Pattern Analysis and Machine Intelligence **14** (2): 239–256.

Blais, G. & Levine, M., 1995: Registering Multi-view Range Data to Create 3D Computer Objects. – IEEE Transactions on Pattern Analysis and Machine Intelligence **17** (8): 239–256.

Chatterjee, S. & Hadi, A.S., 1986: Influential Observations, High Leverage Points, and Outliers in Linear Regression. – Statistical Science **1** (3): 379–393.

Chen, Y. & Medioni, G., 1991: Object Modeling by Registration of Multiple Range Images. – IEEE Conference on Robotics and Automation: 2724–2729, Sacramento, CA, USA.

Filin, S. & Vosselman, G., 2004: Adjustment of airborne laser altimetry strips. – International Archives of Photogrammetry and Remote Sensing **XXXV** (B/3): 285–289, Istanbul, Turkey.

Förstner, W., 1979. Das Programm TRINA zur Trigonometrischen Netzausgleichung. – Nachrichten aus dem öffentlichen Vermessungswesen NRW **2**.

Godin, G., Rioux, M. & Baribeau, R., 1994: Three-dimensional Registration Using Range and Intensity Information. – SPIE Videometrics **III 2350**.

Hampel, F.R., 1974: The Influence Curve and its Role in Robust Estimation. – Journal of the American Statistical Association **69**: 383–393.

Hoaglin, D.C. & Welsch, R.E., 1978: The Hat Matrix in Regression and ANOVA. – The American Statistician **32** (1): 17–22.

Horn, B., Hilden, H. & Negahdaripour, S., 1998: Closed-Form Solution of Absolute Orientation Using Orthonormal Matrices. – Journal of the Optical Society of America **A5** (7): 1127–1135.

Kager, H., 2004: Discrepancies between overlapping laser scanning strips – simultaneous fitting of aerial laser scanner strips. – International Archives of Photogrammetry and Remote Sensing **XXXV** (B/1): 555–560, Istanbul, Turkey.

Kerstling, A.P., Habib, A., Bang, K.-I. & Skaloud, J., 2012: Automated approach for rigorous light detection and ranging system calibration without preprocessing and strict terrain coverage requirements. – Optical Engineering **51**, **076201**.

Kraus, K., 1997: Photogrammetry Vol. 2, Advanced Methods and Applications. – Fourth Edition, 218–220, Dümmler, Bonn.

Maas, H., 2002: Methods for Measuring Height and Planimetry Discrepancies in Airborne Laserscanner Data. – Photogrammetric Engineering and Remote Sensing **68** (9): 933–940.

Masuda, T. & Yokoya, N., 1995: A Robust Method for Registration and Segmentation of Multiple Range Images. – Computer Vision and Image Understanding **61** (3): 295–307.

Planitz, B.M., Maeder, A.J. & Williams, J.A., 2005: The correspondence framework for 3D surface matching algorithms. – Computer Vision and Image Understanding **97** (3): 347–383.

Ressl, C., Mandlburger, G. & Pfeifer, N., 2009: Investigating Adjustment of Airborne Laser Scanning Strips Without Usage of Trajectory Data. – ISPRS Workshop Laser scanning 2009, ISPRS **XXXVIII** (3/W8): 195–200, Paris, France.

Rusinkiewicz, S. & Levoy, M., 2001: Efficient variants of the ICP algorithm. – 3rd International Conference on 3D Digital Imaging and Modeling: 145–152, Quebec, Canada.

Skaloud, J. & Lichti, D., 2006: Rigorous approach to bore-sight self-calibration in airborne laser scanning. – ISPRS Journal of Photogrammetry and Remote Sensing **61** (1): 47–59.

Shakarji, C.M., 1998: Least-squares fitting algorithms of the NIST algorithm testing system. – Journal of Research-National Institute of Standards and Technology **103:** 633–641.

Sharp, G.C., Lee, S.W. & Wehe, D.K., 2002: ICP registration using invariant features. – IEEE Transactions on Pattern Analysis and Machine Intelligence **24** (1): 90–102.

Toth, C.K., 2008: Strip Adjustment and Registration. – Shan, J. & Toth, C.K. (eds.): Topographic Laser Ranging and Scanning: Principles and Processing. – CRC Press.

Address of the Authors:

Philipp Glira, Norbert Pfeifer, Christian Briese & Camillo Ressl, Gusshausstrasse 27–29, A-1040 Vienna, Austria, {philipp.glira}{norbert.pfeifer} {christian.briese}{camillo.ressl}@geo.tuwien.ac.at Tel: +43-(1)-58801-12218, -12219, -12211, -12234, Fax: +43-(1)-58801-12299